Advances in Materials Physics and Chemistry, 2020, 10, 39-52
https://www.scirp.org/journal/ampc
ISSN Online: 2162-5328
ISSN Print: 2162-531X

ArcGIS™ and Principal Component Analysis of Probe Data to Micro-Map Minerals in Round Top Rare Earth Deposit

Lorraine M. Negrón[1], Margaret Piranian[1], Maria A. Amaya[2], Daniel Gorski[3], Nicholas E. Pingitore[1*]

[1]Department of Geological Sciences, The University of Texas at El Paso, El Paso, TX, USA
[2]School of Nursing, The University of Texas at El Paso, El Paso, TX, USA
[3]Texas Mineral Resources Corporation, Sierra Blanca, TX, USA
Email: *npingitore@utep.edu

How to cite this paper: Negrón, L.M., Piranian, M., Amaya, M.A., Gorski, D. and Pingitore, N.E. (2020) ArcGIS™ and Principal Component Analysis of Probe Data to Micro-Map Minerals in Round Top Rare Earth Deposit. *Advances in Materials Physics and Chemistry*, **10**, 39-52.
https://doi.org/10.4236/ampc.2020.102004

Received: December 30, 2019
Accepted: February 18, 2020
Published: February 21, 2020

Abstract

Rare earth elements (REEs), especially heavy rare earth elements (HREEs), are in demand for their current and emerging applications in advanced technologies. Here we perform computer-driven micro-mapping at the millimeter scale of the minerals that comprise Round Top Mountain, in west Texas, USA. This large rhyolite deposit is enriched in HREEs and such other critical elements as Li, Be, and U. Electron probe microanalysis of 2 × 2 mm areas of thin sections of the rhyolite produced individual maps of 16 elements. These were superimposed to generate a 16-element composition at each pixel. Principal components analysis of elements at each pixel identified the specific mineral at that site. The pixels were then relabeled as the appropriate minerals, thereby producing a single mineral map. The overall mineral composition of the 7 studied samples compared favorably with prior analyses of the Round Top deposit available in the literature. Likewise the range of porosity in the maps was consistent with that of previous direct measurements by water saturation. This new statistical and GIS-based technique provides a robust and unbiased approach to electron microprobe mapping. The study further showed that the high-value yttrofluorite grains exhibited little tendency to cluster with other late-stage trace minerals and that the samples extended the previously documented overall homogeneity of the deposit at field scale to this microscopic scale.

Keywords

ArcGIS™, Electron Probe Microanalysis, Principal Component Analysis, Rare Earths, Yttrofluorite, X-Ray Map Analyzer, Round Top

Micro-mapping Round Top Rare Earth Deposit.

1. Introduction

Round Top Mountain, a Tertiary rhyolite laccolith in Hudspeth County, west Texas, USA is a potentially economically valuable deposit of heavy rare earth elements (HREEs) and other critical elements [1]-[10]. The rare earth element (REE) concentrations are over 500 ppm, of which approximately 72% are yttrium and the desirable heavy rare earths (YHREEs), making it a globally significant deposit [3] [7]. Mineralization is homogenous throughout the laccolith with the exception of the rhyolite margins and synchrotron-based X-ray absorption spectroscopy shows that yttrofluorite hosts almost all of the YHREEs [3].

The purpose of this study is to create detailed mineralogical maps from thin sections of Round Top Mountain samples using a new approach that combines multivariate statistical analysis and geospatial analysis through the use of ArcGIS™ [11]. These mineral maps will improve our understanding of the mineralization process at Round Top Mountain and inform approaches to potential extraction of that mineral wealth. This research is an extension of [9] where electron microprobe mapping was used to outline the microscopic distribution of heavy rare earth elements (HREEs) and better understand the mineralization and potential extraction processes.

1.1. Background

Round Top Mountain is a Tertiary rhyolite laccolith in Hudspeth County, Texas, USA. It is a mushroom-shaped, peraluminous igneous intrusion that is roughly 2000 m in diameter and over 375 m high, with a mass estimated at 1.6 billion tons. The rhyolite is composed mainly of Si, O, K, Al, and Na. Round Top Mountain underwent chemical alteration by a late-stage fluorine vapor phase that enriched it in HREEs and other incompatible elements [2] [6] [12]. In the search for and delineation of mineral deposits from Round Top Mountain previous studies [3] [8] [9] have included standard methods such as the collection of rock samples and preparation of thin sections for analysis with optical petrography and scanning electron microscopes. Electron probe microanalysis (EPMA) employs an electron beam excitation to determine the elemental composition of individual grains or portions of grains in thin sections [13]. These analyses confirm the presence of major, minor, and trace elements of potential value within those mineral grains.

The previous study [9] defined the mineral deposits and confirmed the potential resource but they did not provide definitive information on how to extract the desired minerals efficiently and economically. For that reason, we conducted further analyses, including more experimental techniques, to better understand a basis for recovering the HREEs at Round Top Mountain economically.

1.2. Approach

Multivariate statistical techniques, specifically principal component analysis (PCA), were applied to the EPMA intensity maps to define how elements are

spatially correlated and how these clusters represent specific gangue and target minerals. PCA has been used in previous geological studies, for example, to assess the economic potential of a deposit [14], to differentiate between enrichment and pollution of toxic elements in soils [15], and to locate hydrothermal alteration zones associated with metallic deposits [16].

We also use the ArcGIS™ software to analyze the spatial distribution of the chemical elements in the thin sections, expanding on the technique introduced by [11]. ArcGIS™ is widely used in mining applications for geo-spatial analyses, such as mapping ore bodies and minerals [17] and monitoring potential hazards related to mining production [18]. However, [11] first applied the software to X-ray maps from a scanning electron microscope (SEM) equipped with an energy dispersive spectrometer (EDS), along with multivariate statistics, to create multispectral images that illustrated compositional and microtextural relationships in rocks [11]. We utilized their methods to expand the study at Round Top Mountain to produce detailed information on the distribution and associations of minerals at that site.

2. Materials and Methods

2.1. Sample Collection

Texas Mineral Resources Corporation, a publicly traded (stock ticker TMRC) junior mining explorer interested in developing Round Top, contracted an extensive program of reverse circulation drilling to delineate mineralization in the rhyolite. As part of their testing programs, they created a composite sample of several hundred kilograms of material taken from more than 100 drill holes. We chose random pieces from that composite, constrained only by a size, about 2 or 3 cm, large enough to fabricate a petrographic thin section.

2.2. Thin Section Preparation

Samples were cut to provide a mounting surface, then ground flat and glued to a petrographic glass slide. Samples were sliced close to the glass and ground to the standard thickness of 30 μm, using a Buehler PetroThin™ thin section cutter-grinder. The thin sections were polished to a mirror finish, and buffed with a 0.05-μm gamma aluminum oxide powder. Polished thin sections underwent an ultrasonic cleaning bath, an ethanol rinse, and carbon coating prior to analysis. Thin section preparation procedure followed [9].

2.3. Electron Probe Microanalysis

We mapped the elemental composition of our samples on a Cameca SX-50 (upgraded to SX-100 performance) electron probe microanalyser (EPMA) with 4 wavelength dispersive spectrometers (WDS). Instrument settings were 20 KeV electron beam accelerating voltage and 200 or 250 nA current, as imprinted on the images that follow. For each sample a randomly selected 2 × 2 mm area was raster-scanned repeatedly in WDS mode to yield 512 × 512 pixel maps of, indi-

vidually, Fe, K, Al, Si, Nb, Ca, Na, F, Sn, Th, Zr, Rb, Dy, U, Yb, and Y, plus a back scattered electron (BSE) map. The quality of an X-ray map depends on, among other factors, the particular element, its concentration, dwell time of the beam on each pixel, diffracting crystal, detector, and the beam current. Similarly, brightness contrasts in the map depend on the differences in concentration of the element between or within the different phases of any sample. **Figure 1** shows an example of two of these intensity maps obtained for potassium (K) and iron (Fe).

The BSE image displays pixels containing higher atomic number elements (Z) as "bright" areas and those with lower Z elements as darker. Thus average Z within a pixel determines that pixel's relative brightness. The BSE images are helpful for quickly distinguishing different phases. X-ray element maps show the spatial distribution of elements in a sample. Maps of different elements over the same area can help to determine the phases that are present and give a picture of any internal chemical zonation within a mineral.

2.4. X-Ray Map Analyzer

The X-ray Map Analyzer (XRMA) tool developed in Python™ and integrated with ArcGIS™ [11] allows the user to conduct principal component analysis (PCA), with the choice of no filter, a low pass filter, or a focal median filter. Applying different filters to the original X-ray maps can reduce or eliminate background noise, refining the principal components. A low pass filter smoothes the data by taking the mean for each 3 × 3 pixel area. A focal median neighborhood filter takes the shape of a neighborhood (*i.e.*, circle or rectangle) and processes the map cells accordingly. Similar results were obtained using the low pass filter and the rectangular focal median filter. For comparison, we examined the element maps using a low pass filter and a circle focal median filter with a radius of 2 cells.

The greatest asset to using XRMA is that it eliminates decision-making by the user and highlights textural features that are not obvious in optical microscopy or BSE images of thin sections [11].

2.5. Principal Components Analysis

PCA defines a multidimensional coordinate system, where each axis is known as a principal component (PC). PCs can be considered as new super variables that replace sets of variables that are correlated, or in our case, sets of elements that are spatially correlated. In our application, we can consider a PC as likely representing a mineral present in the sample. In general, the largest portion of the information in a data set is found within the first three to five PCs. In our thin sections the first 3 PCs corresponded to the three major minerals found at Round Top. The following PCs described minor and accessory minerals. This paper emphasizes the first 6 PCs due to their importance and relevance to this economic deposit.

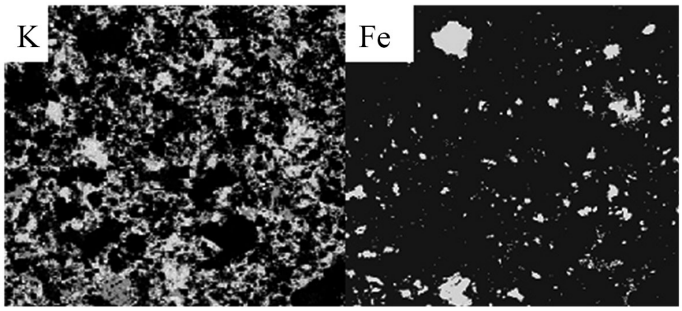

Figure 1. Intensity maps obtained by EPMA of sample RT 10 thin section for elements potassium (left) and iron (right). Brighter areas indicate higher concentrations of the element. Field of View (FOV) 2 × 2 mm.

2.6. ArcGis™

The ArcGIS™ raster calculator tool was used to take multiple individual element X-ray maps such as K, Al, and Si and integrate them to create separate mineral maps, e.g., K-spar, by displaying the pixels in which only those three elements occur together. These individual mineral maps were further refined using the reclassify tool to lower background noise, which narrows the data by labeling pixels with the highest intensity of the mineral with (1) and where it is not, with (0). Refined maps thus are generated delineating only where the mineral is present, and leaving the map blank where the mineral is not present. This allows the analyst to connect the different layers of individual maps and see potential overlapping of minerals or pore space.

2.7. Integrating EPMA, XRMA-PCA, and ArcGIS™

Our overall initial data processing comprised this flow: 1) generate X-ray maps from the EPMA; 2) input the X-ray map into XRMA to determine PCs using no filter, low pass filter, and circle focal median filter; 3) "ground truth" our results by comparing them to mineral compositions obtained in prior published research.

3. Results and Discussion

3.1. Principal Component Analyses

The PCA images generated using the low pass filter yielded the most consistent results and map images overall. Results with no filter appeared noisy and those with the circle focal median filter removed too much of the data. The computer-generated mineral compositions based on the low pass filtered PCA data fall within the range of mineral percentages found in prior research indicating our approach works well. The advantage of the computer-generated approach is that we were able to image smaller minerals and generate a more detailed map of the element locations than previous studies could provide. This is important in analyzing methods for mineral extraction at Round Top Mountain because the principle mineral, yttrofluorite, is typically less than 20 μm in length.

3.2. Principal Components: Major Minerals

In all 7 thin sections the highest weighted variables comprising the first 3 PCs were K, Al, Si, and Na. These four elements are known from bulk elemental analyses [8] [12] to make up approximately 90% or more of Round Top rhyolite. The three minerals corresponding to the first 3 principal components are the major minerals of the Round Top rhyolite: orthoclase feldspar (K-spar, $KAlSi_3O_8$, monoclinic), plagioclase feldspar (albite, $NaAlSi_3O_8$, triclinic) and quartz (SiO_2, trigonal). **Figures 2-4** present X-ray maps for K, Al, Si, and Na, along with larger red-green-blue (RGB) maps of the first 3 principal components, for samples RT 4, RT 7 and RT 9. The X-ray maps, represented on a gray scale, display the highest concentration of the specified element as white.

Note the similarity of the gray areas on the Al and Si maps. These correspond to the similar Al and Si stoichiometries of K-spar and albite. The K map depicts K-spar as rims around black (no K) albite cores. The width of the K-spar rims depends on the size of the albite cores; the smaller the albite core, the wider the K-spar rim, as was observed originally in [1].

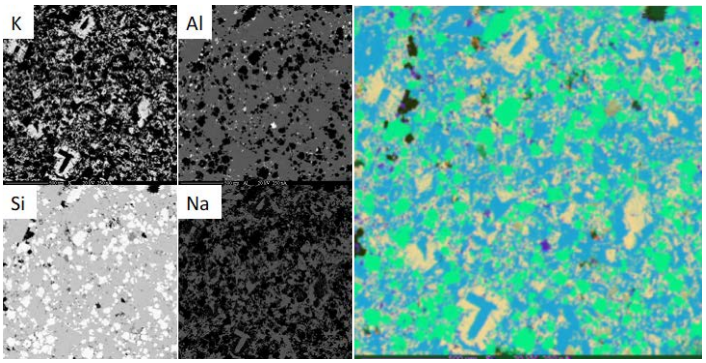

Figure 2. *Top, left to right*: X-ray maps of K and Al. *Bottom, left to right*: X-ray maps of Si and Na in the same area of the petrographic thin section of sample (RT 4) of Round Top Mountain. *Far right*: RGB map of first 3 principal components (R = K-spar, G = Quartz, B = Albite). FOV 2 × 2 mm.

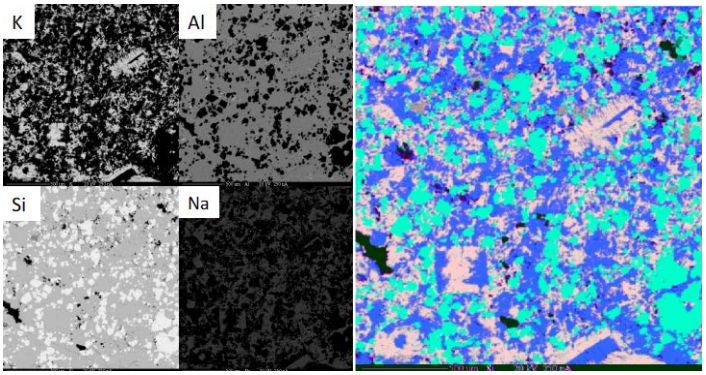

Figure 3. *Top, left to right*: X-ray maps of K and Al. *Bottom, left to right*: X-ray maps of Si and Na in the same area of the petrographic thin section of sample (RT 7) of Round Top Mountain. *Far Right*: RGB map of first 3 principal components (R = K-spar, G = Quartz, B = Albite). FOV 2 × 2 mm.

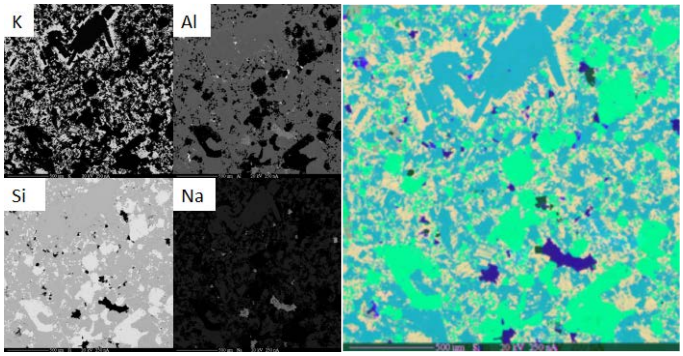

Figure 4. *Top*, *left to right*: X-ray maps of K and Al. *Bottom*, *left to right*: X-ray maps of Si and Na in the same area of the petrographic thin section of sample (RT 9) of Round Top Mountain. *Far right*: RGB map of first 3 principal components (R = K-spar, G = Quartz, B = Albite). FOV 2 × 2 mm.

3.2.1. Potassium Feldspar

PC 1 shows the highest values for potassium, aluminum, and silicon, which corresponds to potassium feldspar (K-spar), $KAlSi_3O_8$. The K map has a close association with rubidium (Rb) for all 7 RT samples. Monovalent rubidium, an alkali metal, commonly substitutes for its alkali neighbor potassium in the K-spar structure. With respect to the RGB map (**Figure 2**) the pink outlines the location of K-spar, which in the average of our 7 samples comprises 51 volume percent (vol%) of the rhyolite (**Table 1**), nearly identical to the 52 vol% and 48 - 52 vol% of the earlier studies [1] [4].

3.2.2. Quartz

PC 2 shows a peak high value of silicon, which corresponds to the mineral quartz, SiO_2, for 6 out of 7 RT samples. **Figures 2-4** depict the quartz grains in green. Quartz makes up approximately 23 vol% of the composition of the rhyolite (**Table 1**), a value somewhat lower than the 30 vol% and 28 - 30 vol% in the prior estimates [1] [4].

3.2.3. Albite

PC 3 also displays high values for silicon, followed by aluminum and sodium (albite-$NaAlSi_3O_8$). Albite phenocrysts are located in blue within the RGB map. Albite comprises 13 vol% (**Table 1**), consistent with the earlier 11 vol% and 8% - 14% [1] [4].

3.3. Principal Components: Minor and Accessory Minerals

The minor minerals annite mica, magnetite, and zircon comprise 7% - 10% of the rhyolite. The accessory minerals yttrofluorite, columbite, thorite, and cassiterite are seen in all 7 samples in trace amounts.

3.3.1. Annite Mica

Annite mica corresponds to high loadings for Fe, Si, and Al with minor loadings of Dy (an EPMA artifact due to an overlap of X-ray emissions with Fe), F, U and Yb. The Fe map has gray shades that align well with Al and Si, consistent with

Table 1. Comparison of round top mineral compositions.

	Volume % of Mineral		
Mineral	This Study	Rubin *et al.* 1987 [1]	O'Neill 2014 [4]
K-Spar	52	51	48 - 52
Quartz	23	30	28 - 30
Albite	13	11	8 - 14
Mica	4.3	4.5	4 - 5
Magnetite/Hematite	2.1	1	2 - 3
Cryolite	1.2	2.5	
Zircon	0.32	Trace	
Yttrofluorite	0.25	Trace	

the composition of an Fe-rich biotite, annite ($KFe_3^{2+}AlSi_3O_{10}(OH,F)_2$, monoclinic). The mica found within the thin sections averages 4.3 vol% (Table 1), close to the 4.5 vol% and 4 - 5 vol% of the earlier studies [1] [4].

3.3.2. Magnetite

The brightest areas on the EPMA Fe X-ray maps are assumed to be magnetite (Fe_3O_4, isometric), and possibly some hematite. Magnetite percentages fall within the range from 1% to 4.8% in the rhyolite samples. Table 1 shows magnetite at 2.1 vol%, consistent with the 1 vol% and 2 - 3 vol% in the prior studies [1] [4].

3.3.3. Yttrofluorite

The rare earth elements (REEs) yttrium, ytterbium, and dysprosium are among the high value economic target elements in the Round Top Mountain deposit. Dy, Y, and Yb grains correspond with one another and are incorporated in yttrofluorite. The target mineral yttrofluorite (YF), the most valuable mineral in the deposit, is present in very small amounts. Yttrofluorite (Ca, Y, HREE)F_2, isometric) is a variety of fluorite (CaF_2, isometric) where up to approximately 30% of the Ca^{2+} is substituted for by Y and other mostly HREEs. Yttrofluorite averaged 0.25 vol% (Table 1).

3.3.4. Zircon

One of the minor minerals that shows up as a principal component describes where zirconium (Zr) and silicon (Si) have the highest loadings. These elements combined, as minerals, define the mineral zircon ($Zr(SiO_4)$, tetragonal) This mineral was present at the 0.32 vol% level (Table 1).

3.3.5. Cryolite

The 7th and 8th principal component consistently displays high loadings for sodium (Na), fluorine (F), and aluminum (Al). These elements combined, as a mineral, describe the mineral cryolite (Na_3AlF_6, monoclinic). The mineral percent composition for cryolite was 1.2 vol%, somewhat lower than the 2.5 vol% in [1].

3.3.6. Columbite

One of the accessory minerals shows up as a principal component in high load-

ings for niobium (Nb), ytterbium (Yb), and iron (Fe). These elements together, as an oxide, describe the mineral columbite ($Fe^{2+}Nb_2O_6$ to $Mn^{2+}Nb_2O_6$, orthorhombic). Columbite vol% averaged 0.3%.

3.3.7. Thorite

The 14th principal component consistently displays high loadings for thorium (Th), uranium (U), and silicon (Si). These elements combined describe the mineral thorite ($Th(SiO_4)$, tetragonal). Thorite was present at 0.1 vol%.

3.3.8. Uraninite

The 15th principal component consistently displays high loadings for uranium (U). This element combined with oxygen, as a mineral, describes the mineral uraninite (UO_2), isometric. This mineral was present at the 0.1 vol% level.

3.3.9. Cassiterite

Another accessory mineral displays high loadings for tin (Sn). This element, as an oxide, describes the mineral cassiterite (SnO_2, tetragonal). The mineral cassiterite comprised 0.02 vol% of the rhyolite.

3.4. Evaluation of Comparison of Results with Those of Earlier Studies

To test the validity of the combined PCA and Arc GISTM methods the previous section and **Table 1** compared our computer-generated composition (averages of 7 samples) to published mineralogical results from earlier studies [1] [4]. The first study [1] converted their bulk chemical (elements) analysis of a Round Top sample to a mineral composition *via* the CIPW norm, a long-established method in petrology. The CIPW calculation originated with the need to estimate the mineral composition of an aphanitic igneous rock (one so fine-grained that the minerals could not be point counted with a petrographic microscope) from its bulk elemental composition, based on chemical analysis [19]. The earlier study provided a table with normative volume percents of the main minerals. These can be compared directly to our results, which are based on measurements of the area occupied by the different minerals in the thin sections, area and volume percents being equivalent. Our results were systematically adjusted upwards by 3% to reflect the estimated effect of pore space on the mineral composition, which was not measured in the bulk elemental analysis of [1].

The compositional ranges from the second comparative study [4] were based on microscopic examination of thin sections from nearly 50 samples. These data were presented as volume percents, based on occupied areas in the thin sections.

As anticipated, there was general agreement between the studies, suggesting that our approach is valid (**Table 1**). But note that this test is an imperfect one. The earlier studies collected surface samples from the deposit. These might have been altered by proximity to country rock during emplacement of the laccolith or been subjected to weathering in their surficial environment. Our samples

were from drill cuttings and likely are more representative of the actual bulk of the deposit. Further, we must emphasize that the actual overall composition of the laccolith is both unknown and unknowable, and all attempts to characterize that composition are limited by sampling and analytical considerations.

The similarities among the studies emphasize the earlier finding that the mineralization at Round Top is remarkably homogeneous [8]. That earlier geochemical study involved some 1400 samples from more than 100 drill holes spread across the mountain. That represents homogeneity at a scale of tens to hundreds of meters. Here we compared our seven 2 × 2 mm sampling areas, examined by electron probe microanalysis to a depths of a few micrometers, to a mineralogy analysis based on bulk elemental chemistry [1] and analysis of numerous full thin sections [4]. This suggests that the Round Top Mountain rhyolite composition is homogeneous for many elements down to the mm scale. Viewed another way, the electron probe analysis for most of the elements extended less than 10 μm into the sample. Thus, the total analyzed mass in our study was minuscule, likely some 700 *micrograms!*

3.5. Mineralogical Textural Analysis: Major and Minor Elements

Figure 5 presents mineral maps of samples RT 2 and RT 12. The K-spar (pink) phenocrysts found in these two samples range in size between 50 and 250 μm in length. The K-spar surrounds the albite cores (light gray) as rims; the albite ranges from 20 to 100 μm in length. The location of the quartz is indicated in yellow and is seen dispersed randomly throughout the thin sections. The quartz grains range from 20 to 150 μm and are anhedral to subhedral in appearance. Magnetite (black) and annite biotite (brown) are both found dispersed throughout, with phenocrysts ranging between 10 and 100 μm in length. Also present are such minor or accessory minerals as zircon, cryolite, yttrofluorite, cassiterite, columbite, uraninite and thorite, although these minerals are present in trace amounts and thus they are not depicted here.

3.6. Mineralogical Textural Analysis: Yttrofluorite Distribution

To discern which minerals neighbor the valuable target yttrofluorite we overlaid the YF map on top of maps of the major and minor minerals (**Figure 6**). Zooming into individual YF grains, approximately 1 - 20 μm in length, those neighbors could be determined. Six out of the seven mineral maps showed that the majority of the YF grains were associated with K-spar and quartz grains. Occasionally, the YF grains abut albite grains and, less commonly, the iron-rich phases, magnetite or annite mica. RT 10 exhibited a different behavior in which the YF grains are solely found on the Fe-rich mica (annite).

We had expected that perhaps the YF would be clustered adjacent to, or in discrete micro-pods with, other minerals containing incompatible elements that were precipitated contemporaneously with the YF in the late-stage fluorine mineralization event. This does not appear always to have been the case, with most

of the yttrofluorite isolated from, and some associated with the minor and accessory minerals. Concentration of the valuable YF with such other potential targets as columbite-tantalite, cassiterite, zircon, and uraninite would have suggested that fine grinding and mechanical separation of such clusters could be an economically viable approach to exploiting this multi-mineral deposit.

3.7. Mineralogical Textural Analysis: Porosity

Figure 7 shows sample RT 4, a pink rhyolite, with a pulled out section of the upper right-hand corner enlarged in order to highlight this porosity. The black areas are the pore spaces found between minerals. Each pixel is approximately 4 μm in size.

Previous studies have shown that Round Top Mountain rhyolites have 1% to 2% porosity in the gray varieties and 3% - 8% porosity in the pink varieties [5]. This porosity is evident in the mineral maps. Using ArcGIS™, the percentage of pore spaces was calculated to range from 1.4% to 4.0% in the 7 samples, consistent with earlier measurements of porosity by water saturation [5].

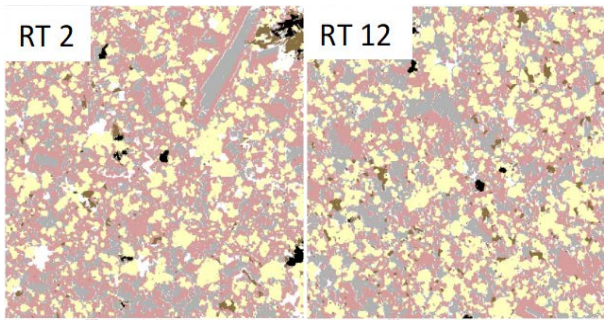

Figure 5. Mineral maps of thin sections of samples RT 2 and RT 12. K-spar (pink), albite (light gray), quartz (yellow), magnetite (black), annite mica (brown). FOV 2 × 2 mm.

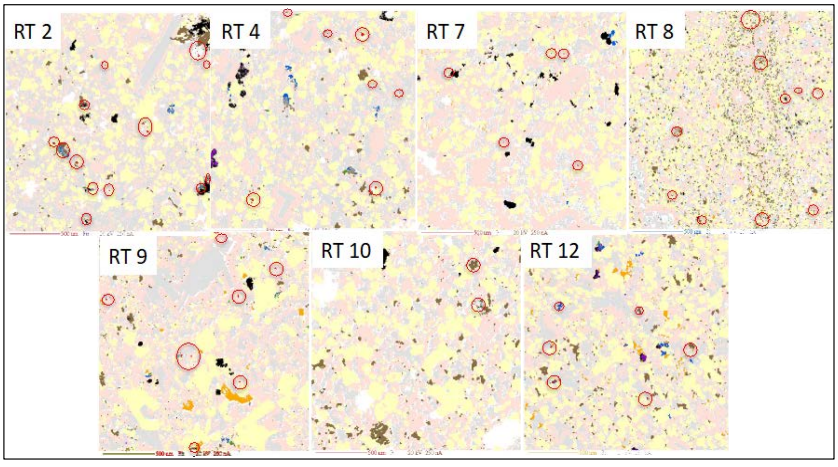

Figure 6. All 7 RT mineral maps with major, minor, and accessory minerals, K-spar (pink), albite (10% gray), quartz (yellow), magnetite (black), annite mica (brown), zircon (blue), cryolite (orange), uraninite (40% gray), thorite (purple), cassiterite (light blue), columbite (green), and yttrofluorite (red and circled). FOV 2 × 2 mm.

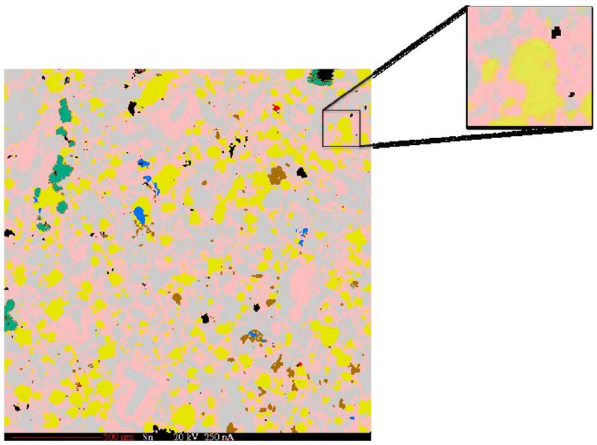

Figure 7. Mineral map of sample RT 4 showing pore space (black areas). FOV 2 × 2 mm.

4. Conclusion

Multivariate analysis was performed on seven thin sections of Round Top Mountain rhyolite. Through the use of the XRMA tool package in ArcGIS™, principal components were derived and percentages of major and minor minerals were determined. By overlaying the X-ray element maps in ArcGIS™, element-mineral correlations were observed for each principal component at each pixel. This enabled conversion of the elemental maps into mineral maps. Resulting overall mineralogy proved consistent with results from prior investigations. This new approach presents the opportunity to use computer-generated information to provide an unbiased basis for creation of mineralogical maps from elemental maps. The study further demonstrated the overall homogeneity of the Round Top Mountain deposit at the microscopic scale.

Acknowledgements

The authors thank Texas Mineral Resources Corporation for providing access to proprietary technical data and samples. This project was supported by joint research contracts 26-8211-12 and 26-8211-16 between TMRC and the University of Texas at El Paso. Funds to cover the costs to publish in open access were obtained from this source. Also, we thank Prof. Gaetano Ortolano and Ph.D. candidate Roberto Visalli from the University of Catania, Italy for access to their X-ray Map Analyzer application.

Disclosure

M.P., M.A., and L.N. declare no potential conflicts and received no compensation for project participation. D.G. is the CEO of TMRC and serves on its Board of Directors. N.P. serves on the Board of Directors of TMRC. He is not and has never been an employee of TMRC, nor has he received any compensation from the research contracts that supported this research. The funding sponsor, TMRC, had no role in the decision to publish the results.

Conflicts of Interest

The authors declare no conflicts of interest regarding the publication of this paper.

References

[1] Rubin, J.N., Price, J.G., Henry, C.D. and Koppenaal, D.W. (1987) Cryolite-Bearing and Rare Metal-Enriched Rhyolite, Sierra Blanca Peaks, Hudspeth County, Texas. *American Mineralogist*, **72**, 1122-1130.

[2] Price, J.G, Rubin J.N., Henry, C.D., Pinkston, T.L., Tweedy, S.W. and Koppenaal, D.W. (1990) Rare-Metal Enriched Peraluminous Rhyolites in a Continental Arc, Sierra Blanca Area, Trans-Pecos Texas; Chemical Modification by Vapor-Phase Crystallization. *GSA Special Papers*, **246**, 103-120. https://doi.org/10.1130/SPE246-p103

[3] Pingitore Jr., N.E., Clague, J.W. and Gorski, D. (2014) Round Top Mountain (Texas, USA) a Massive, Unique Y-Bearing-Fluorite-Hosted Heavy Rare Earth Element (HREE) Deposit. *Journal of Rare Earths*, **32**, 90-96. https://doi.org/10.1016/S1002-0721(14)60037-5

[4] O'Neill, L.C. (2014) REE-Be-U-F Mineralization of the Round Top Laccolith, Sierra Blanca Peaks, Trans-Pecos Texas. MSc Thesis, University of Texas at Austin, Austin.

[5] Negrón, L., Pingitore Jr., N.E. and Gorski, D. (2016) Porosity and Permeability of Round Top Rhyolite (Texas, USA) Favor Coarse Crush Size for Rare Earth Element Heap Leach. *Minerals*, **6**, 16. https://doi.org/10.3390/min6010016

[6] Elliott, B.A., O'Neill, L.C. and Kyle, J.R. (2017) Mineralogy and Crystallization History of a Highly Differentiated REE-Enriched Hypabyssal Rhyolite: Round Top Laccolith, Trans-Pecos, Texas. *Mineralogy and Petrology*, **111**, 569-592. https://doi.org/10.1007/s00710-017-0511-5

[7] Jowitt, S.M., Medlin, C.C. and Cas, R.A.F. (2017) The Rare Earth Element (REE) Mineralisation Potential of Highly Fractionated Rhyolites: A Potential Low-Grade, Bulk Tonnage Source of Critical Metals. *Ore Geology Reviews*, **86**, 548-562. https://doi.org/10.1016/j.oregeorev.2017.02.027

[8] Pingitore Jr., N.E., Clague, J.W. and Gorski, D. (2018) Remarkably Consistent Rare Earth Element Grades at Round Top Yttrofluorite Deposit. *Advances in Materials Physics and Chemistry*, *Special Issue*: *Rare Earth Elements*, **8**, 1-14. https://doi.org/10.4236/ampc.2018.81001

[9] Pingitore Jr., N.E., Piranian, M., Negrón, L. and Gorski, D. (2018) Microprobe Mapping of Rare Earth Element Distribution in Round Top Yttrofluorite Deposit. *Advances in Materials Physics and Chemistry*, *Special Issue*: *Rare Earth Elements*, **8**, 15-31. https://doi.org/10.4236/ampc.2018.81002

[10] Elliott, B.A. (2019) Petrogenesis of Heavy Rare Earth Element Enriched Rhyolite: Source and Magmatic Evolution of the Round Top Laccolith, Trans-Pecos, Texas. *Minerals*, **8**, 423. https://doi.org/10.3390/min8100423

[11] Ortolano, G., Zappalà, L. and Mazzoleni, P. (2014) X-Ray Map Analyser: A New ArcGIS™® Based Tool for the Quantitative Statistical Data Handling of X-Ray Maps (Geo- and Material-Science Applications). *Computers & Geosciences*, **72**, 49-64. https://doi.org/10.1016/j.cageo.2014.07.006

[12] Gustavson Associates (2019) NI 43-101 Preliminary Economic Assessment: Round Top Project, Sierra Blanca, Texas.

http://tmrcorp.com/_resources/reports/TMRC-NI43-101-PEA-2019-16-August-2019.pdf

[13] Khashgerel, B., Kavalieris, I. and Hayashi, K. (2008) Mineralogy, Textures, and Whole-Rock Geochemistry of Advanced Argillic Alteration: Hugo Dummett Porphyry Cu-Au Deposty, Oyu Tolgoi Mineral District, Mongolia. *Mineralium Deposita*, **43**, 913-932. https://doi.org/10.1007/s00126-008-0205-3

[14] Rambert, F. (2005) Introduction to Mining Geostatistics. *Conference Proceedings*, 67*th EAGE Conference & Exhibition*, Madrid, 13-16 Jun 2005, cp-140-00030. https://doi.org/10.3997/2214-4609.201405201

[15] Borůvka, L., Vacek, O. and Jehlička (2005) Principal Component Analysis as a Tool to Indicate the Origins of Potentially Toxic Elements in Soils. *Geoderma*, **128**, 289-300. https://doi.org/10.1016/j.geoderma.2005.04.010

[16] Crósta, A.P., De Souza Filho, C.R., Azevedo, F. and Brodie, C. (2003) Targeting Key Alteration Minerals in Epithermal Deposits in Patagonia, Argentina, Using ASTER Imagery and Principal Component Analysis. *International Journal of Remote Sensing*, **24**, 4233-4240. https://doi.org/10.1080/0143116031000152291

[17] Sprague, K., de Kemp, E., Wong, W., McGaughey, J., Perron, G. and Tucker, B. (2006) Spatial Targeting Using Queries in a 3-D GIS Environment with Application to Mineral Exploration. *Computers & Geosciences*, **32**, 396-418. https://doi.org/10.1016/j.cageo.2005.07.008

[18] Gasser, R., Knežević, G. and Carrier, M. (2015) Mine Risk Management by Mapping. *Journal of ERW and Mine Action*, **15**, Article 21, 46-49.

[19] https://en.wikipedia.org/wiki/Normative_mineralogy